Published in final edited form as:
Gastrointest Endosc. 2008 October ; 68(4): 737–744. doi:10.1016/j.gie.2008.05.018.

High-resolution imaging in Barrett's Esophagus: a novel, low-cost endoscopic microscope

Timothy J. Muldoon, B.S., **Sharmila Anandasabapathy, M.D.**, **Dipen Maru, M.D.**, and **Rebecca Richards-Kortum, Ph.D.***
Houston, TX USA

Abstract

Background—This report describes the clinical evaluation of a novel, low-cost, high-resolution endoscopic microscope for obtaining fluorescent images of the cellular morphology of the epithelium of regions of the esophagus with Barrett's metaplasia. This noninvasive point imaging system offers a method for obtaining real-time histological information during endoscopy.

Objective—The objective of this study is to compare images taken with the fiber-optic endoscopic microscope with standard histopathology.

Design—Feasibility study

Setting—The University of Texas M.D. Anderson Cancer Center Department of Gastroenterology.

Patients, Interventions, and Main Outcome Measurements—The tissue samples studied in this report were obtained by endoscopic resection from patients with previous diagnoses of either high grade dysplasia or esophageal adenocarcinoma.

Results—Three distinct tissue types were observed *ex vivo* with the endoscopic microscope: normal squamous mucosa, Barrett's metaplasia, and high grade dysplasia. Squamous tissue was identified by bright nuclei surrounded by dark cytoplasm in an ordered pattern. Barrett's metaplasia could be identified by large glandular structures with intact nuclear polarity. High grade dysplasia was visualized as plentiful, irregular glandular structures and loss of nuclear polarity. Standard histopathology of study samples confirmed the results obtained by the endoscopic microscope.

Limitations—The endoscopic microscope probe had to be placed into direct contact with tissue.

Conclusions—It was feasible to obtain high-resolution histopathologic information using the endoscopic microscope device. Future improvement and integration with wide field endoscopic techniques will aid in improving the sensitivity of detection of dysplasia and early cancer development in the esophagus.

*Contact information for corresponding author: rkortum@rice.edu, Rice University, Department of Bioengineering, MS 142, 6100 Main St, Keck Hall #116, Houston, TX 77005.

Contributions: conception and design (S.A. and R.R.K.); analysis and interpretation of the data (all authors); drafting of the article (T.M.); critical revision of the article for important intellectual content (T.M., S.A., R.R.K); final approval of the article (S.A. and R.R.K).

Current affiliations: Rice University Department of Bioengineering, Houston, TX USA (T.J.M and R.R.K.), The University of Texas M.D. Anderson Cancer Center, Department of Gastroenterology, Houston, TX USA, (S.A.), and The University of Texas M.D. Anderson Cancer Center, Department of Pathology, Houston, TX USA (D.M.)

Keywords

Barrett's Esophagus; Esophageal Adenocarcinoma; Optical Biopsy; High-Resolution Imaging; Fluorescence imaging

Introduction

Barrett's Esophagus (BE) is characterized by the replacement of the normal squamous epithelium of the esophagus by a specialized, metaplastic columnar mucosa. A result of chronic gastroesophageal reflux disease, BE is significant because of a drastically increased risk for the development of esophageal adenocarcinoma (EAC). Indeed, subjects with BE carry a risk of EAC up to 125 times greater than the average person[1]. EAC itself is one of the most rapidly rising cancers in the United States having undergone a 5 to 10% increase in incidence per year over the last 30 years2, 3. Despite increased awareness, survival rates for EAC remain a dismal 10-25%, an outcome largely due to diagnosis at an advanced stage.

In an effort to improve these statistics, much work has been focused on the early detection of EAC, through the diagnosis of high-grade dysplasia or minimally invasive (intramucosal) adenocarcinoma. However, the detection of this early neoplasia is technically challenging. On standard white-light endoscopy, dysplasia and early EAC are often focal, flat and difficult to consistently distinguish from regular metaplasia. Moreover, the current standard of esophagogastroduodenoscopy (EGD) with random, 4-quadrant biopsies has been shown to miss nearly 2/3 of dysplastic lesions4-6. Therefore, there is a demand for minimally-invasive techniques which can detect dysplasia or cancer at an early stage. Such early detection will not only improve survival rates, but also facilitate the application of less-morbid alternatives to esophagectomy, such as endoscopic mucosal resection (EMR).

Several recent optical technologies have sought to increase the detection of neoplasia, at both low and high-resolution. Among the lower resolution (so-called 'widefield' technologies), autofluorescence endoscopy (AF) and narrow-band imaging (NBI) have been the best studied to date. While both of these modalities, have been shown to increase the detection of high grade dysplasia and early adenocarcinoma, specificity has not been impressive[7-13]. This is in part due to esophagitis and inflammatory confounders and other reactive epithelial alterations which can increase the number of false-positives.

In order to improve upon current specificity rates among these new endoscopic imaging modalities, the use of complementary high-resolution technologies, capable of subcellular imaging, has been proposed. One of the most promising of these high-resolution techniques is confocal endomicroscopy[14]. Indeed, a recent study by Kiesslich et al. found high sensitivity and specificity rates for the detection of HGD/intramucosal EAC, when a confocal endoscope was used with fluorescent contrast agents[15, 16]. While use of such a device may be ideal in an academic or tertiary care-setting where the prevalence of neoplasia is high, cost and the necessity for a separate system may preclude its translation to the community. Indeed, in a community-based, average-risk surveillance setting, a low-cost, probe-based device, compatible with any standard endoscope, may be preferable.

In this paper, we describe a novel, low-cost imaging device developed in our laboratory. Our endoscopic microscope is based on the use of a flexible, small-caliber, fiber-optic image guide bundle. This fiber bundle, 1 millimeter in diameter, can be inserted into the biopsy channel of any standard endoscope, and is capable of fluorescence imaging at subcellular resolution[17]. Perhaps most appealing is the fact that the current prototype consists of less than $2500 in components and uses a 1-2 mm outer diameter probe which can be inserted into the biopsy

channel of an endoscope, then sterilized and reused. This further reduces the cost of each application of the device, making it an ideal technology for community-based application.

Patients and Methods

Patients

Patients who participated in this study had been previously diagnosed with either high-grade dysplasia or intramucosal adenocarcinoma, and were scheduled for upper endoscopy with either jumbo biopsies or endoscopic mucosal resection (EMR) of the affected areas. The study protocols were approved by both the Rice University Institutional Review Board and the University of Texas M.D. Anderson Cancer Center Institutional Review Board, and informed consent was obtained from each patient before the procedure. Eleven sequential patients with a documented history of Barrett's esophagus were approached for enrollment. One patient was excluded due to inability to perform the EMR (non-lifting); the remaining ten were imaged using the endoscopic microscope and topical acriflavine.

For each patient, there were typically one to two samples obtained, and approximately 5 to 10 measurement sites on each sample. Images presented in this paper are typical for high quality specimens.

Methods

For this study, EMR specimens or 4 mm jumbo biopsies were obtained by a single endoscopist (S.A.) from patients with Barrett's dysplasia or esophageal adenocarcinoma. Optical images were obtained immediately after application of topical acriflavine (see Contrast Agent). Following imaging, the EMR samples and biopsies were submitted to a single expert GI pathologist (D.M.) for interpretation and the optical and histopathologic images reviewed. Over 100 optical images were obtained and reviewed.

The Fiber Bundle Microscope

The endoscopic microscope used in this study consisted of a 3 meter long image guide with 30,000 individual fibers. The spacing of the individual fibers largely determines the spatial resolution of the endoscopic microscope; in this case, the center-to-center spacing was approximately 4 microns. The field of view of the system depends on the diameter of the active area of the fiber bundle; in this case, a circular field of view with a diameter of 750 microns was produced. Images were produced by placing the distal surface of the fiber bundle into direct contact with the tissue to be interrogated. The image guide can be easily passed through the biopsy port of a standard endoscope (Fig. 1). Illumination was provided by a blue LED centered at 455 nm, which produced an illumination intensity of approximately 1 mW at the distal end of the fiber bundle. Fluorescent light returning through the bundle was directed to a scientific-grade CCD camera coupled to a PC. Images are displayed at a typical frame rate of 2 to 4 frames per second. The images presented in this paper appear as they would to a clinician viewing the monitor in a real-time setting.

Fluorescent Contrast Agent

Acriflavine hydrochloride was used as a topical contrast agent and was applied to tissues prior to imaging. Acriflavine has been shown to localize to the nuclei of cells, with minimal nonspecific cytoplasmic staining. A solution of 0.05% (w/v) acriflavine in buffered saline was applied with a cotton swab to the mucosa of each EMR specimen or biopsy prior to imaging. The acriflavine was placed on the specimen for 30 seconds, which was then rinsed with buffered saline to eliminate any unbound dye. Imaging was performed immediately following labeling.

Criteria for interpretation of images

The criteria applied to interpret endoscopic microscope images were based on differential histologic characteristics of tissue. These include well-established features seen on light microscopy of standard histologic sections and previously published criteria for scanning confocal microscopy[15, 18]. The criteria used for light microscopy and confocal microscopy were utilized to identify the tissue type and evaluate the architectural and cytologic alterations.

The non-neoplastic squamous mucosa is identified on histologic sections by its flat multilayered arrangement with polyhedral cell shapes, well defined cell membranes and centrally situated nuclei with regular internuclear distances. The invaginating lamina propria (papillae) are identified as extensions of lamina propria- composed of loose connective tissue with thin walled blood vessels- into the squamous epithelium at regular intervals. On confocal microscopy the cytologic characteristics of squamous epithelium is essentially identical to histology with polygonal cell shapes with well defined cell membranes and centrally situated nuclei; the latter two identified by their bright color as compared to the darker cytoplasm. Flat multilayering is assessed by the unaltered shape of the epithelial arrangement at progressively deeper optical sections of the mucosa. The papillae are identified as a circular dark area with the presence of scattered small bright structures corresponding to the connective tissue, red blood cells and inflammatory cells. The presence of intraepithelial inflammation is identified by inflammatory cells, which are seen as bright oval to round structures which are haphazardly distributed in the epithelium.

Barrett's esophagus (intestinal metaplasia) is identified on histology by the presence of villiform architecture, columnar enterocytes and goblet cells. The criteria used for confocal microscopy includes the presence of round double layer ring (torus) structures which alter their shapes at different optical thicknesses. At deeper levels the ring-like structures show the classic villiform architecture. The villi are lined by the columnar enterocytes with bight nuclei and dark cytoplasm. The lamina propria in the core of the villi shows a similar appearance to the squamous papillae with blood vessels and inflammatory cells. At cellular levels the presence of goblet cell is identified by clear to dark blue globules admixed with the columnar enterocytes. The border of the goblet cells is particularly bright in good quality images. In non-dysplastic Barrett's mucosa the intervillous stroma is abundant and identified by the presence of loose connective tissue, inflammatory cells and blood vessels. In highly dysplastic Barrett's mucosa the villous architecture is either effaced or completely lost. In addition, at different optical thicknesses the architecture is uniform with complex back-to-back arrangements of small glandular structures with minimal intervening stroma. The cytologic alterations, like multilayering of the cells, bright nuclear appearance, decreased goblet cells and high nuclear-to-cytoplasmic ratios are also applied to identify high-grade dysplasia. Another feature seen in good quality images is the structural relation of epithelium and subepithelial capillaries. In non dysplastic Barrett's mucosa the capillaries are regular and seen at upper and mid level thicknesses. However, in highly dysplastic mucosa the capillaries are seen only at deeper levels and show variations in size and shape.

Each image was analyzed independently and in a blinded fashion by both a gastrointestinal pathologist and a gastroenterologist. Endoscopic microscope images were then correlated with the standard histopathologic images, previously interpreted by the GI pathologist.

Results

Images obtained with the endoscopic microscope were compared to histopathologic interpretation of the same areas. Fluorescence images were evaluated qualitatively, noting nuclear size and density, nuclear-to-cytoplasmic ratio, glandular structure and organization, and intensity of fluorescence. Distinct patterns of fluorescence images were observed for

tissues with different histopathologic diagnoses: (1) normal squamous epithelium, (2) Barrett's metaplasia/low grade dysplasia, and (3) Barrett's neoplasia (high grade dysplasia or intramucosal adenocarcinoma).

Normal Squamous Tissue

Figure 2 shows histologic and endoscopic fluorescence microscopy images of normal squamous mucosa obtained from a site which appeared normal on white light endoscopy. The biopsy fragment was also imaged with a commercial fiber optic confocal endoscope (Pentax/Optiscan), and a standard commercial benchtop confocal system (Zeiss LSM 510 Meta). Both the fiber optic confocal system and the benchtop confocal microscope used an excitation wavelength of 488 nm.

Individual cell nuclei are easily visible as discreet bright dots in fluorescence images obtained with the endoscopic microscope and the two confocal systems (Fig. 2). The field of view of the endoscopic microscope is much larger than the two confocal systems while the spatial resolution is somewhat decreased In addition, the frame rate of the endoscopic microscope (2 to 4 frames per second) is faster than that of the commercially available confocal endoscope (0.8 frames per second). The squamous epithelium is distinguished by its multilayering, polyhedral/polygonal shape and centrally situated nuclei and well defined cell membrane. Uniform spacing of the nuclei indicates the intact polarity which distinguishes benign squamous mucosa. This also helps in differentiating other, more randomly distributed cells (e.g. inflammatory cells) which might infiltrate the epithelium.

Barrett's metaplasia

Endoscopic microscope imaging was performed at several sites on EMR specimens labeled topically with acriflavine. Two sites are described in this paper (Fig. 3). The endoscopic microscope image in Fig. 3a shows glandular epithelium characterized by double ring-like architecture with bright density distributed uniformly along the basement membrane consistent with intact nuclear polarity. In addition, the nuclei are uniformly distributed in the epithelium away from the basement membrane. These features are consistent with non-dysplastic glandular mucosa.

The image in Fig. 3b shows similar features as Fig. 3a except for a small area of focal complex architecture, the significance of which is uncertain as the nuclear arrangement is that of non-dysplastic glandular epithelium described in Fig. 3a This image is also consistent with Barrett's without dysplasia. The hematoxylin-eosin stained section of the same specimen in Fig. 3c shows distinctive type Barrett's mucosa, histologically defined as intestinal metaplasia. The intestinal metaplasia is characterized by the presence of goblet cells, easily identified by intracytoplasmic clear-to-light blue vacuoles. These features are consistent with Barrett's metaplasia.

High grade dysplasia

Endoscopic microscopy and histopathologic images taken from an EMR specimen with HGD are shown in Fig. 4a and b, respectively. Fig. 4a shows a confluent proliferation of small glandular structures with variable size and shape with occasional areas showing a gland-in-gland appearance. High nuclear density along with a large component of cells occupied entirely by nuclei indicate high nuclear-to-cytoplasmic ratio. These features are consistent with high-grade dysplasia.

The hematoxylin-eosin stained section of the specimen shows distinctive type Barrett's mucosa with high-grade dysplasia, consistent with the features observed in the fluorescence image. The high-grade dysplasia is characterized by architecturally complex arrangement of the glands

and loss of nuclear polarity, nuclear overcrowding, and nuclei and mitotic figures reaching up to the luminal surface.

Discussion

This study demonstrates the ability of an inexpensive (< $2500) system with a reusable probe to produce high-resolution images of a variety of esophageal tissue types. Such a device can easily be integrated into any standard endoscope to non-invasively yield subcellular-resolution images of the surface histology of a suspected lesion with the use of an appropriate fluorescent dye. Coupled with wide-field imaging devices, this endoscopic microscope system should further enhance specificity for detection of Barrett's neoplasia. This low-cost device has advantages over more complex ‘optical biopsy’ systems because of its easy application to a wide variety of settings and platforms. The probe itself can be disinfected and reused, further reducing the cost of each use of the device. Moreover, the straightforward optical design is highly robust and requires no scanning mirrors or other moving parts, enabling such technology to disseminate to areas with high levels of support as well as regions with less infrastructure and resources.

Non-invasive visualization of the cellular architecture enables a clinician to more thoroughly inspect the mucosa, and diagnose and treat intraepithelial neoplasia immediately. The strength of our study is the application of well-established, age-old pathologic criteria to interpret the optical images. Ideally, the real-time interpretation of such images will involve close collaboration between a gastroenterologist and GI pathologist. As has been shown with the interpretation of confocal endomicroscopic images, gastroenterologists can be trained to interpret optical images and distinguish 2 pathologic classifications: Barrett's metaplasia/low grade dysplasia and Barrett's high grade dysplasia/intramucosal adenocarcinoma. A larger study with robust kappa statistics for interobserver reproducibility is planned for validation of this concept with this device. Additionally, work is underway to develop algorithms based on standard pathologic criteria (nuclear:cytoplasmic ratio, etc.) which can be translated into rapid, real-time, image-processing and interpretation software.

From a clinical management standpoint, the diagnosis of Barrett's HGD or intramucosal adenocarcinoma is the most critical distinction. Given the large interobserver variability in the interpretation of low-grade dysplasia and the subtle architectural and morphologic features which characterize LGD, we feel that the identification of LGD may be beyond the capabilities of this technology. However, given the low likelihood of progression of LGD, we do not believe this is significant drawback. To further enhance the sensitivity and specificity of the technology for the detection of HGD/intramucosal cancer, we are currently working on combining high-resolution fluorescence imaging with other molecular-specific techniques (eq. optical contrast agents targeted to epithelial biomarkers).

In order to achieve the high frame rates and good image quality seen in images from this device, selection of a bright, selective fluorescent dye is critical. Acriflavine hydrochloride, previously used as a topical antiseptic, was chosen for its ability to cross cell membranes and label acid molecules, including DNA. Acriflavine has been used in a number of European and Australian *in vivo* imaging studies of the gastrointestinal epithelium, as well as other studies, without any reported adverse effects[16, 19-21]. While acriflavine displays some affinity for collagen and elastin and some residual staining occurs in the cytoplasmic regions of cells, strong contrast is observed between cell nuclei and the surrounding cytoplasm. This enables qualitative observation of the cellular architecture of squamous and glandular patterns, as well as providing an estimate of nuclear-to-cytoplasmic ratios. Topical acriflavine also stains only the superficial layers of tissue, and has been shown to have limited effect below the lamina propria[16]. Since the contact imaging procedure used in the endoscopic microscope does not perform optical

sectioning and does not reject fluorescent light as efficiently as a confocal microscope, superficial labeling improves image detail.

There have been recent advances in the use of molecular-specific contrast agents. These agents consist of an optical reporter conjugated to a monoclonal antibody, aptamer, or other targeting ligand, and have been successfully implemented for the detection of abnormal expression levels of cell surface markers, including epidermal growth factor receptor (EGFR)[22]. These fluorescent contrast agents can be used with existing high-resolution point imaging devices to yield both qualitative and quantitative data about the nature of neoplastic disease. In addition, the response of a particular tumor to a given therapy could be monitored over time in a non-invasive fashion.

In conclusion, we have developed a **low-cost** fiber bundle-based high-resolution imaging system which is capable of visualizing cellular architecture, morphology, and nuclear-to-cytoplasmic ratios. Preliminary *ex vivo* evaluation shows that this system can differentiate between squamous mucosa, Barrett's metaplasia, and Barrett's intraepithelial neoplasia. Through the use of image processing techniques and segmentation of individual cell nuclei in images collected from the endoscopic microscope, it will be possible to provide a quantitative estimate of nuclear-to-cytoplasmic ratios[17]. Future development and automation of such image processing software will lead to objective surveillance algorithms that can assist the endoscopist in locating dysplastic lesions. The use of such a translatable system in concert with existing and developing wide-field endoscopic technologies may facilitate improved specificity for the detection of Barrett's neoplasia and further clinical evaluation of this technology is forthcoming.

Acknowledgments

The authors gratefully acknowledge support from NIH/NIDDK Center Grant P30 DK56338 and the Texas Digestive Disease Center (Dr. Anandasabapathy) and NIH grants RO1 EB002179 and BRP CA103830 (Dr. Richards-Kortum).

Special appreciation is extended to Rachna Khare and Carolyn Paraguya for their expertise and assistance.

References

1. Williamson WA, Ellis FH Jr, Gibb SP, Shahian DM, Aretz HT, Heatley GJ, Watkins E Jr. Barrett's esophagus. Prevalence and incidence of adenocarcinoma. Arch Intern Med 1991;151:2212–6. [PubMed: 1953225]
2. DeVault KR. Epidemiology and significance of Barrett's esophagus. Dig Dis 2000;18:195–202. [PubMed: 11356990]
3. Cameron AJ. Epidemiology of Barrett's esophagus and adenocarcinoma. Dis Esophagus 2002;15:106–8. [PubMed: 12220415]
4. Thomson BNJ, Cade RJ. Oesophagectomy for early adenocarcinoma and dysplasia arising in Barrett's oesophagus. Anz Journal of Surgery 2003;73:121–124. [PubMed: 12608973]
5. Dellon ES, Shaheen NJ. Does screening for Barrett's esophagus and adenocarcinorna of the esophagus prolong survival? Journal of Clinical Oncology 2005;23:4478–4482. [PubMed: 16002837]
6. van Sandick JW, van Lanschot JJB, Kuiken BW, Tytgat GNJ, Offerhaus GJA, Obertop H. Impact of endoscopic biopsy surveillance of Barrett's oesophagus on pathological stage and clinical outcome of Barrett's carcinoma. Gut 1998;43:216–222. [PubMed: 10189847]
7. Egger K, Werner M, Meining A, Ott R, Allescher HD, Hofler H, Classen M, Rosch T. Biopsy surveillance is still necessary in patients with Barrett's oesophagus despite new endoscopic imaging techniques. Gut 2003;52:18–23. [PubMed: 12477753]
8. Curvers WL, Wong LM, Song K, Wang KK, Gostout CJ, Wallace MB, Wolfson HC, Ragunath K, Fockens P, Ten Kate FJ, Krishnadath KK, Bergman JJ. Endoscopic tri-modal imaging (ETMI) for the detection of dysplastic lesions in Barrett's Esophagus. Gastroenterology 2006;130:A642–a642.

9. Kara M, DaCosta RS, Wilson BC, Marcon NE, Bergman J. Autofluorescence-based detection of early neoplasia in patients with Barrett's esophagus. Digestive Diseases 2004;22:134–141. [PubMed: 15383754]
10. Kara M, Ennahachi M, Fockens P, Peters F, ten Kate F, Bergman J. Narrow-band imaging (NBI) in Barrett's esophagus (BE): What features are relevant for the detection of high-grade dysplasia (HGD) and early cancer (EC)? Gastroenterology 2004;126:A50–a50.
11. Hamamoto Y, Endo T, Nosho K, Arimura Y, Sato M, Imai K. Usefulness of narrow-band imaging endoscopy for diagnosis of Barrett's esophagus. Journal of Gastroenterology 2004;39:14–20. [PubMed: 14767729]
12. Ross AS, Noffsinger A, Waxman I. Narrow band imaging directed EMR for Barrett's esophagus with high-grade dysplasia. Gastrointestinal Endoscopy 2007;65:166–169. [PubMed: 17185100]
13. Niepsuj K, Niepsuj G, Cebula W, Zieleznik W, Adamek M, Sielanczyk A, Adamczyk J, Kurek J, Sieron A. Autofluorescence endoscopy for detection of high-grade dysplasia in short-segment Barrett's esophagus. Gastrointestinal Endoscopy 2003;58:715–719. [PubMed: 14595307]
14. Yoshida S, Tanaka S, Hirata M, Mouri R, Kaneko I, Oka S, Yoshihara M, Chayama K. Optical biopsy of GI lesions by reflectance-type laser-scanning confocal microscopy. Gastrointestinal Endoscopy 2007;66:144–149. [PubMed: 17591488]
15. Kiesslich R, Gossner L, Goetz M, Dahlmann A, Vieth M, Stolte M, Hoffman A, Jung M, Nafe B, Galle PR, Neurath MF. In vivo histology of Barrett's esophagus and associated neoplasia by confocal laser endomicroscopy. Clin Gastroenterol Hepatol 2006;4:979–87. [PubMed: 16843068]
16. Polglase AL, McLaren WJ, Skinner SA, Kiesslich R, Neurath MF, Delaney PM. A fluorescence confocal endomicroscope for in vivo microscopy of the upper- and the lower-GI tract. Gastrointest Endosc 2005;62:686–95. [PubMed: 16246680]
17. Muldoon TJ, P MC, Nida DL, Williams MD, Gillenwater A, Richards-Kortum R. Subcellular-resolution molecular imaging within living tissue by fiber microendoscopy. Optics Express 2007;15:16413–16423. [PubMed: 19550931]
18. Inoue H, Cho JY, Satodate H, Sakashita M, Hidaka E, Fukami S, Kazawa T, Yoshida T, Shiokawa A, Kudo S. Development of Virtual Histology and Virtual Biopsy Using Laser-scanning Confocal Microscopy. Scan J Gastroenterol 2003;38:37–39.
19. Kiesslich R, Burg J, Vieth M, Gnaendiger J, Enders M, Delaney P, Polglase A, McLaren W, Janell D, Thomas S, Nafe B, Galle PR, Neurath MF. Confocal laser endoscopy for diagnosing intraepithelial neoplasias and colorectal cancer in vivo. Gastroenterology 2004;127:706–13. [PubMed: 15362025]
20. Pitten FA, Kramer A. Antimicrobial efficacy of antiseptic mouthrinse solutions. Eur J Clin Pharmacol 1999;55:95–100. [PubMed: 10335902]
21. Mathe G. The failure of HAART to cure the HIV-1/AIDS complex. Suggestions to add integrase inhibitors as complementary virostatics, and to replace their continuous long combination applications by short sequences differing by drug rotations. Biomed Pharmacother 2001;55:295–300. [PubMed: 11478579]
22. Ke S, Wen X, Gurfinkel M, Charnsangavej C, Wallace S, Sevick-Muraca EM, Li C. Near-infrared optical imaging of epidermal growth factor receptor in breast cancer xenografts. Cancer Res 2003;63:7870–5. [PubMed: 14633715]

Acronym List

BE	Barrett's Esophagus
EAC	Esophageal adenocarcinoma
EMR	Endoscopic mucosal resection
EGD	Esophagogastroduodenoscopy
AF	Autofluorescence endoscopy
NBI	Narrow-band imaging
HGD	High grade dysplasia

LED	Light-emitting diode
DNA	Deoxyribonucleic acid
EGFR	Epidermal growth factor receptor

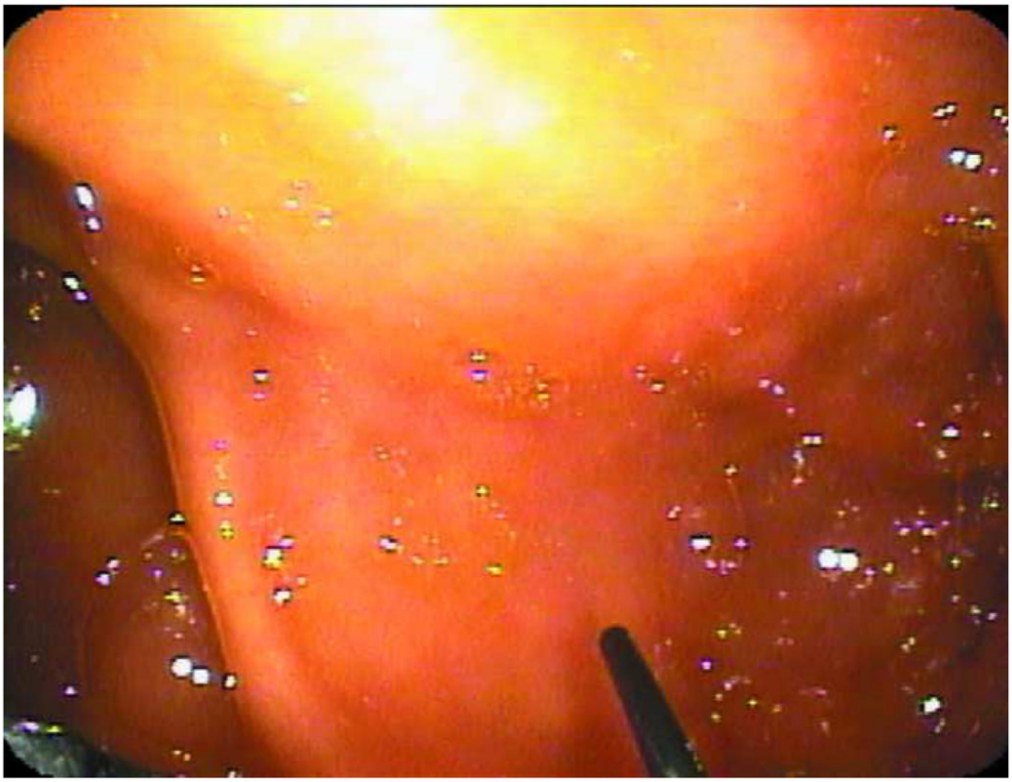

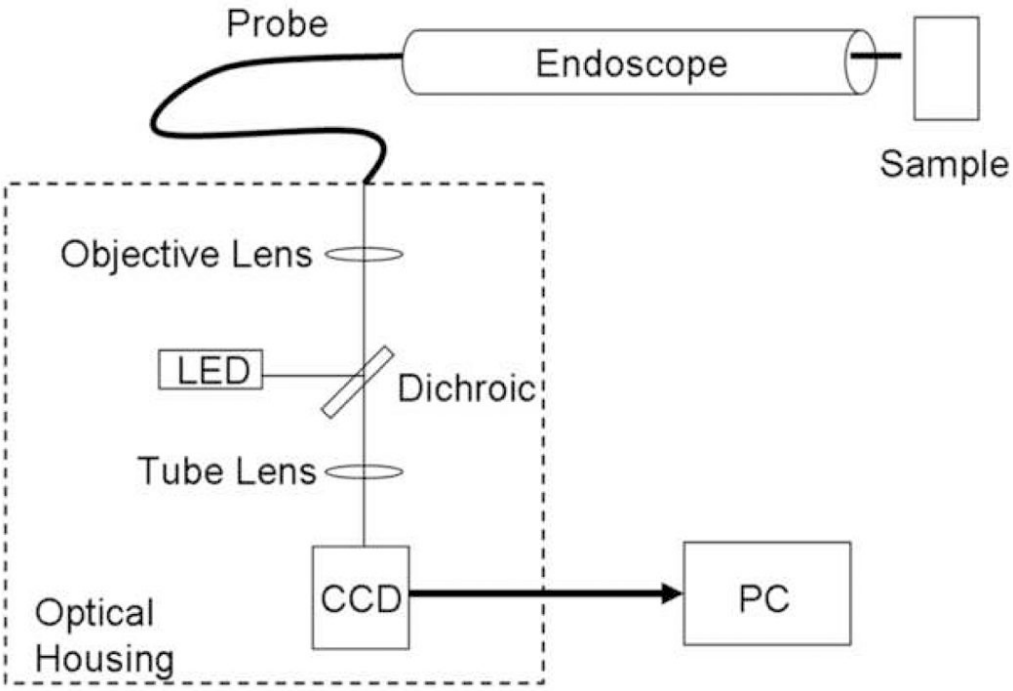

Figure 1.
Endoscopic Microscope. **A**. Image of fiber bundle extending through the biopsy port of a standard white-light endoscope. **B**. Image of fiber bundle probe *in vivo.* **C**. Image of table-top endoscopic microscope; fluorescence microscope unit is on the left, data-acquisition PC is on the right. **D**. Schematic overview of the system.

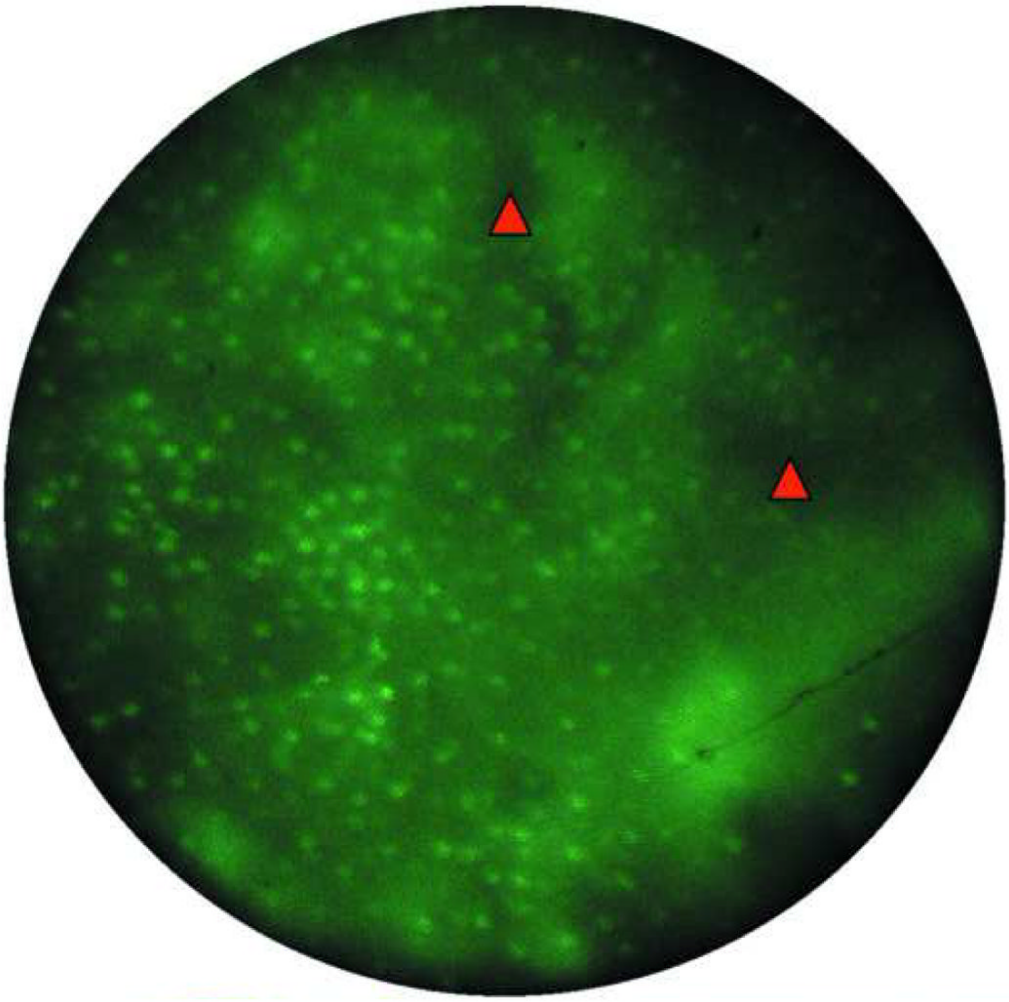

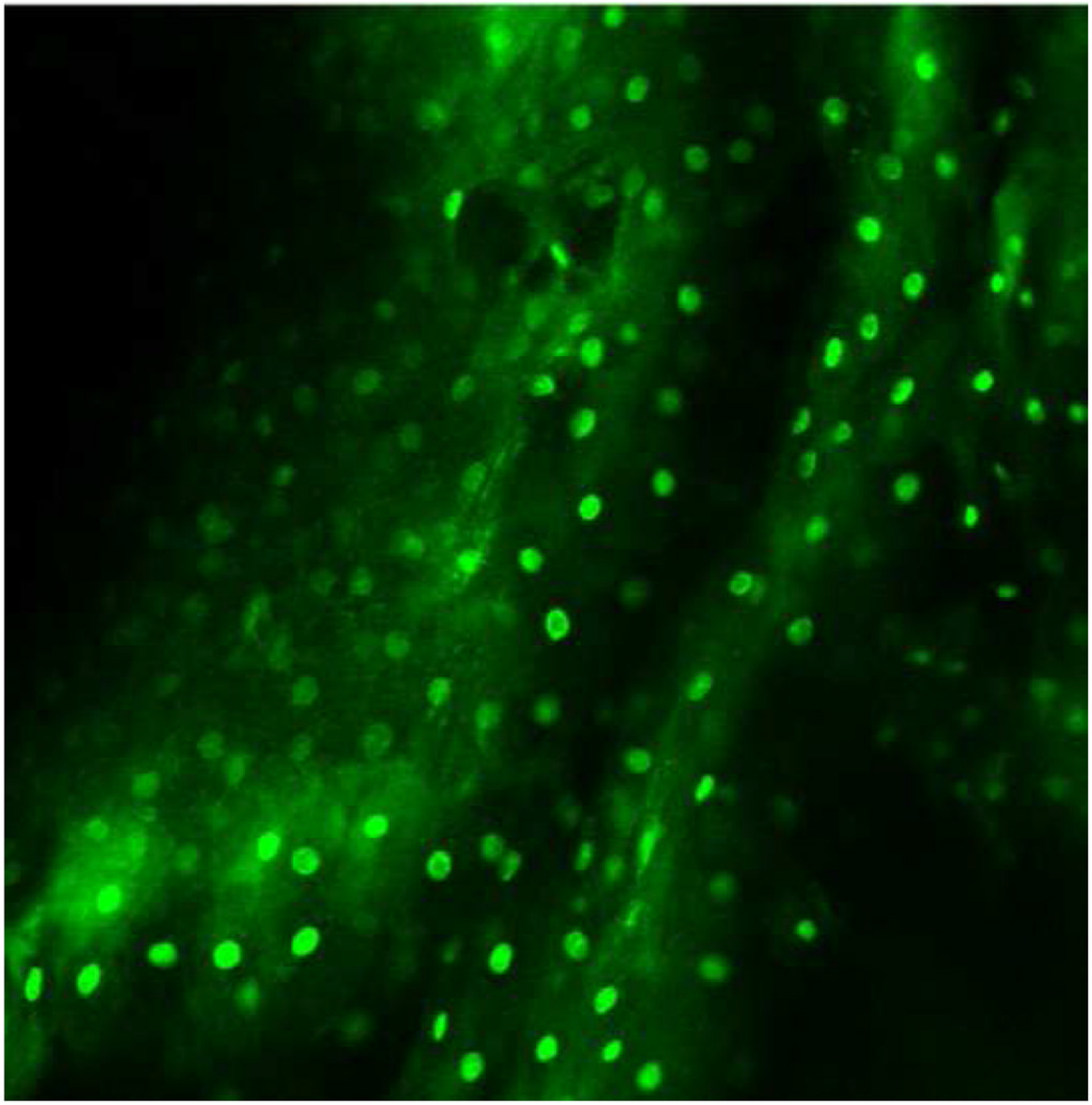

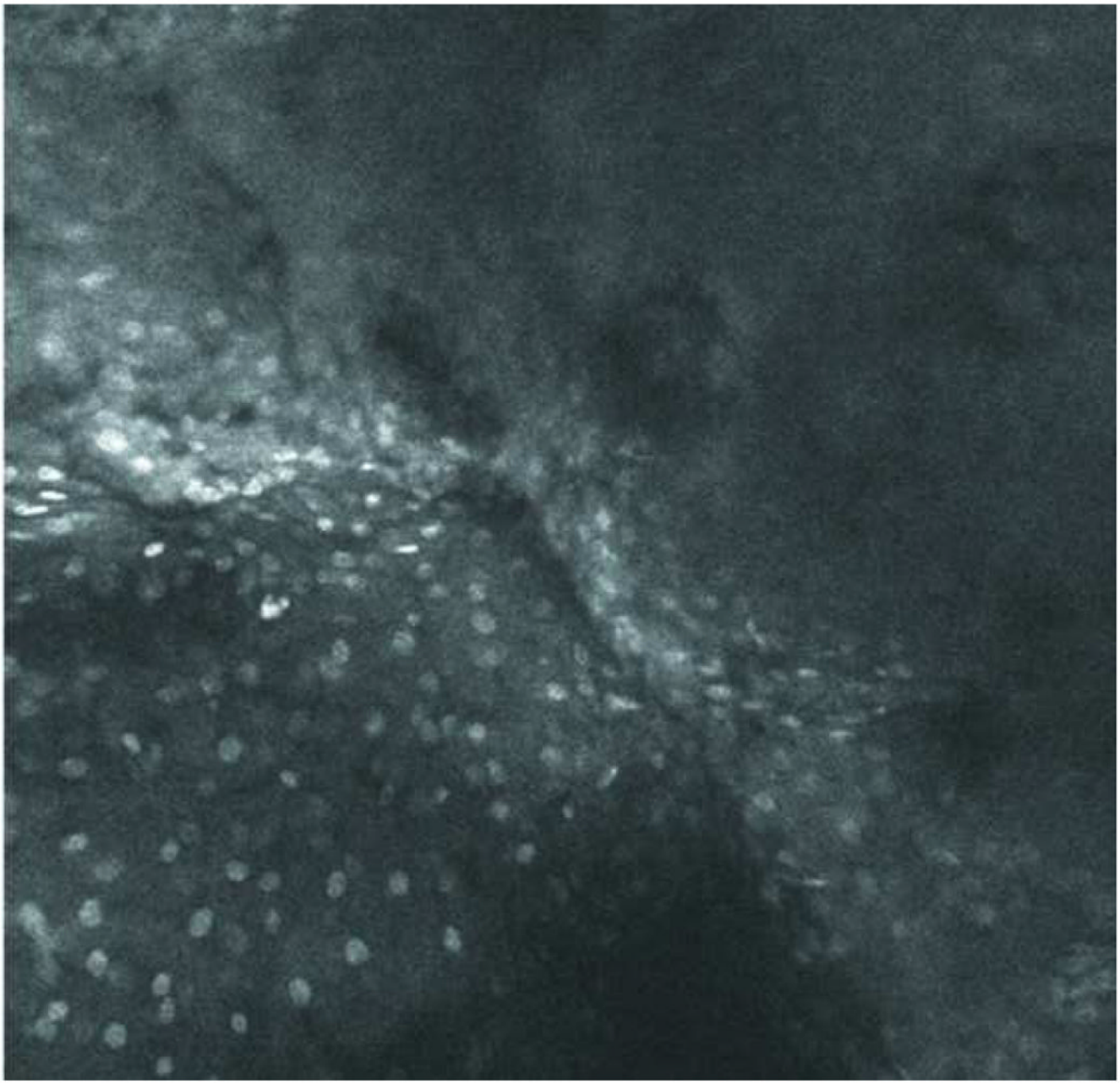

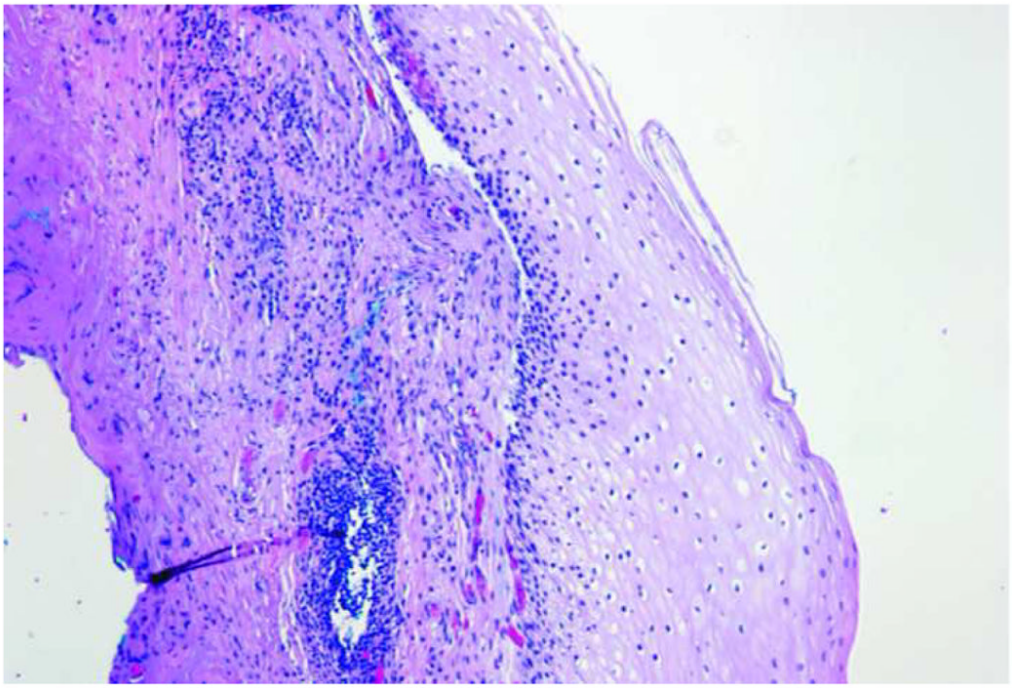

Figure 2.

Images of normal squamous tissue. **A**. Endoscopic microscope image of normal squamous tissue stained with 0.05% acriflavine. **B**. Benchtop confocal (Zeiss LSM 510 Meta) image of same tissue. **C**. Pentax endoscopic confocal image of same tissue. **A-C** show flat arrangement of squamous epithelium with round regularly spaced nuclei. The round clear spaces surrounded by the epithelium represent the papillae (red arrowhead). The acriflavine in image **A** highlights the nuclei. **D**. Histopathology of same specimen. Scale bar is 100 microns.

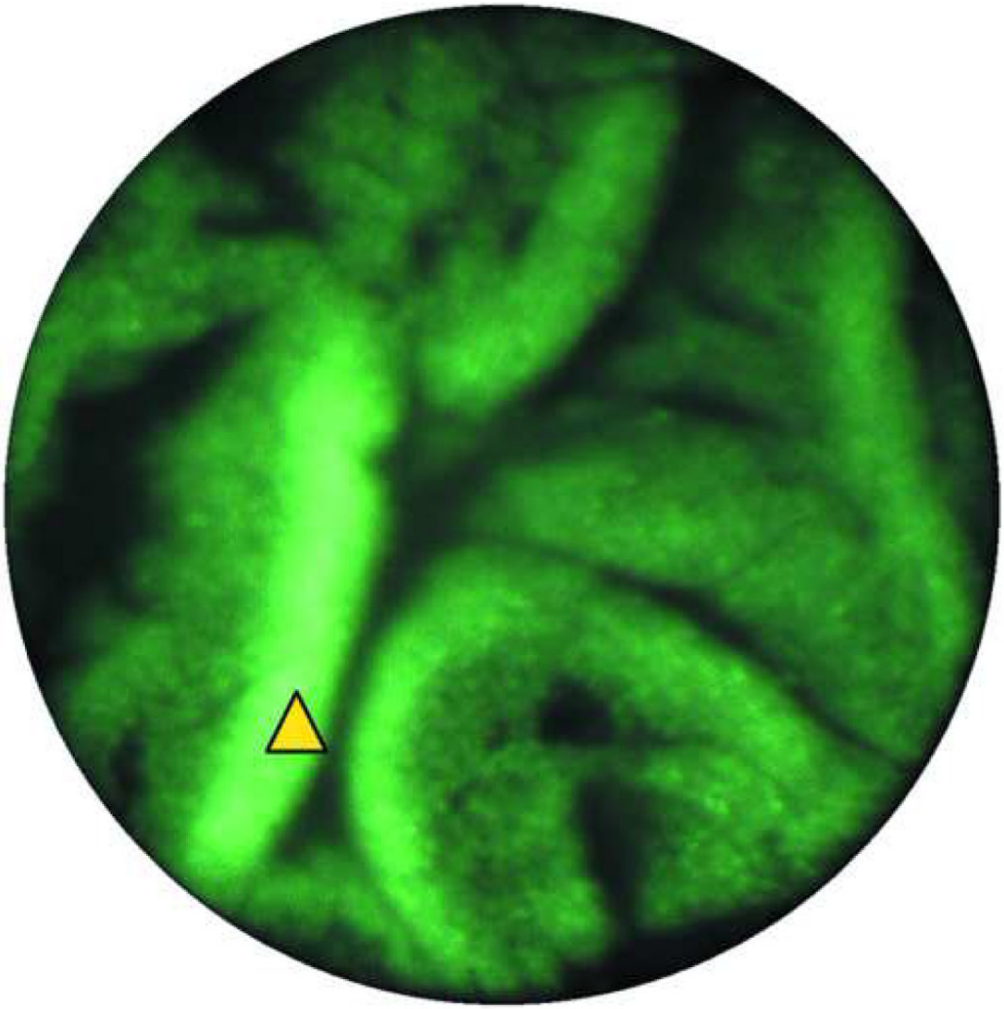

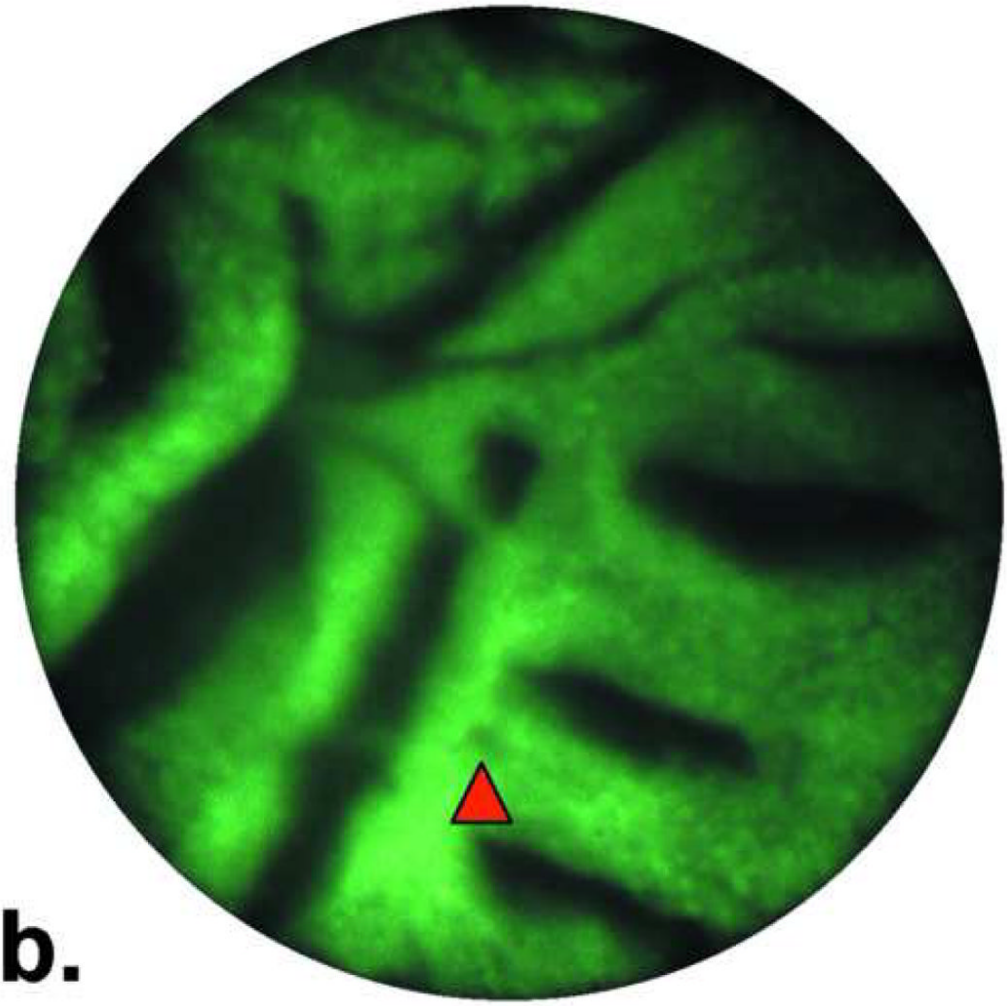

b.

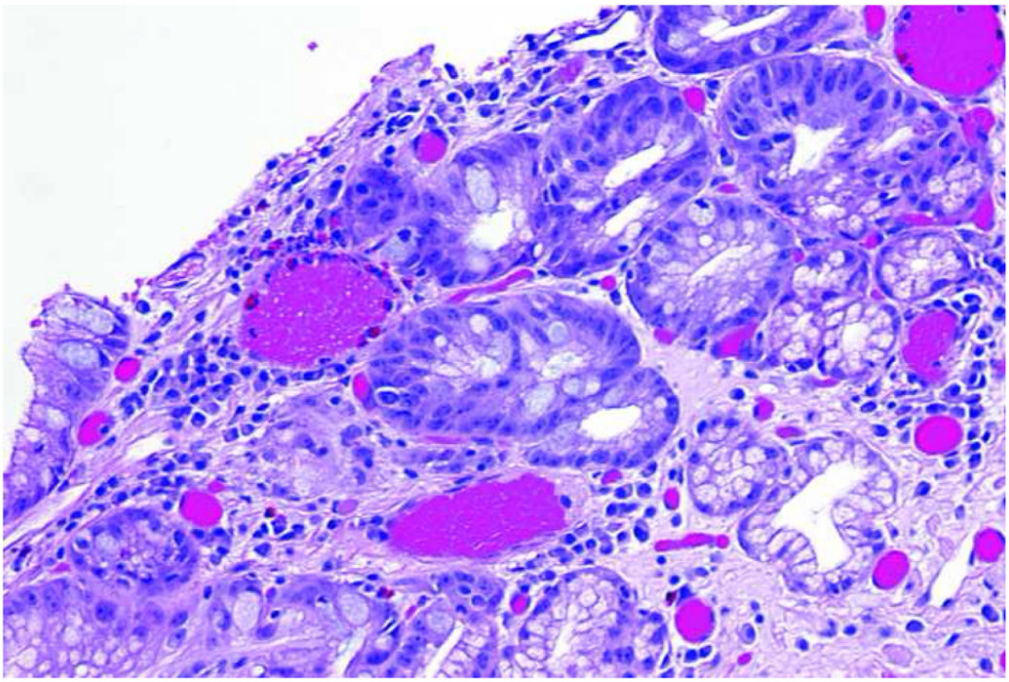

Figure 3.
Images of Barrett's metaplasia. **A**. and **B**. Endoscopic microscope of Barrett's metaplasia stained with 0.05% acriflavine. Image **A** shows broad villous architecture. The bright band at the base of each villous-like structure indicates the high uptake of acriflavine by the nuclei (yellow arrowhead). Image **B** shows larger torus-like structures with intervening stroma. Occasional goblet cells are highlighted by a marker (red arrowhead). **C**. Histopathology of same sample. Scale bars are 100 microns; all images at the same scale.

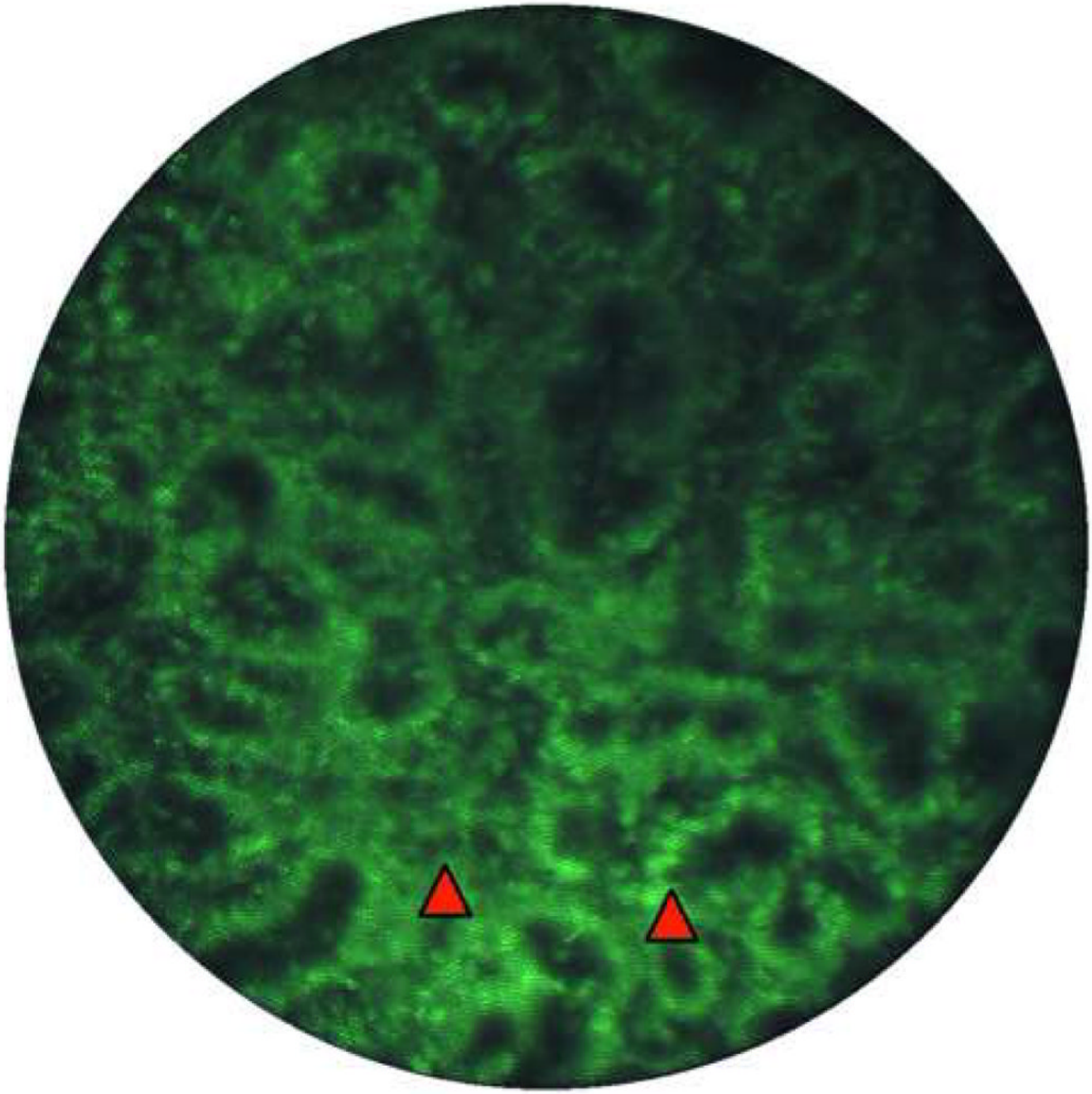

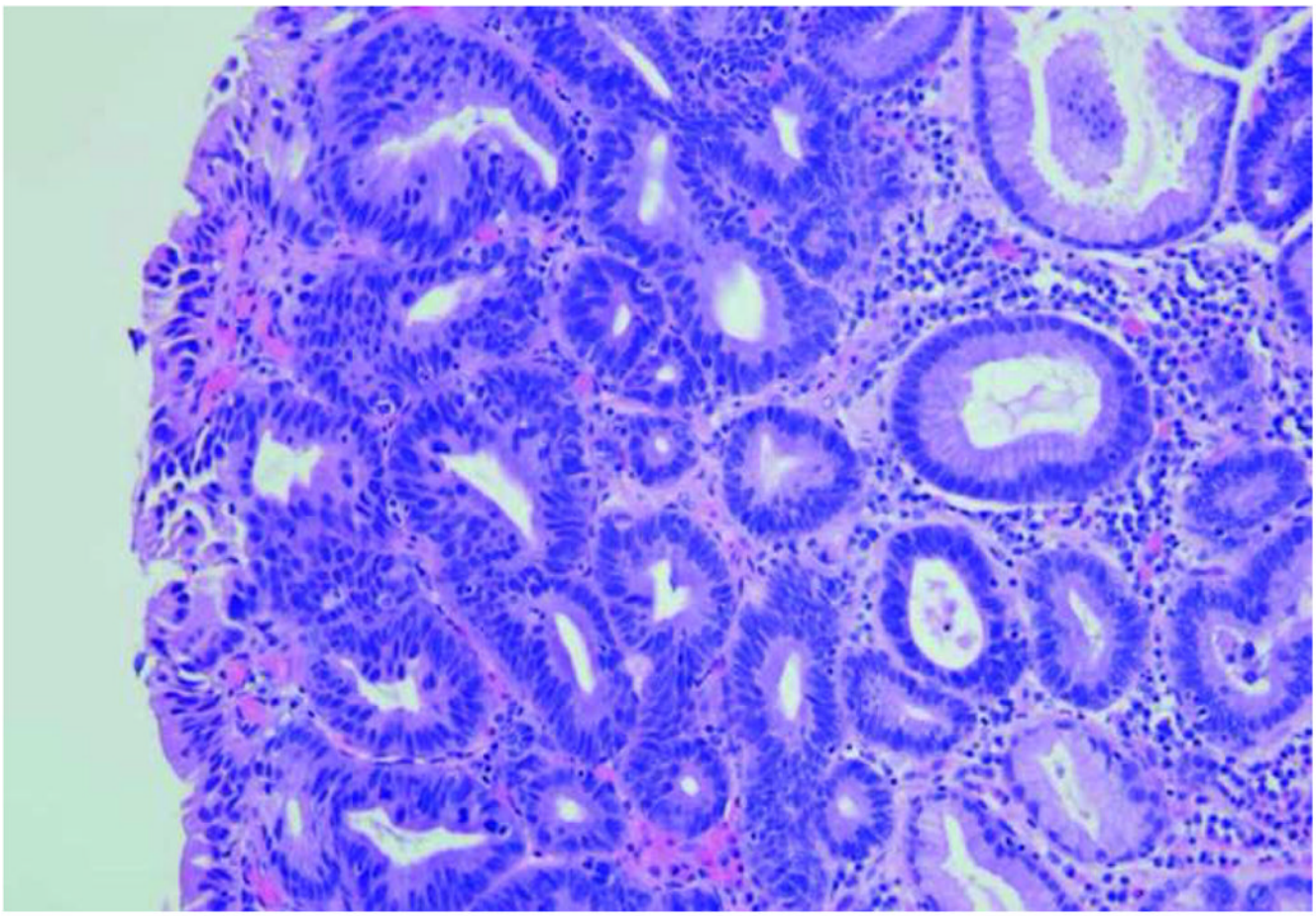

Figure 4.
Image of high-grade dysplasia. **A**. Endoscopic microscope image of high grade dysplasia stained with 0.05% acriflavine. Confluent and haphazard glandular proliferation with back–to-back arrangements and minimal to absent stroma. Foci of high nuclear intensity and high nuclear–to-cytoplasmic ratio are highlighted by markers (red arrowheads). **B**. Histopathology of same specimen. Scale bar is 100 microns; all images are at the same scale.